TAO, Vol.3, No.4, 469-482, December 1992

ESTIMATION OF Q VALUE BY SP/S SPECTRAL RATIO

CHIOU-FEN SHIEH*

(Received: March 2, 1992; Revised: October 2, 1992)

ABSTRACT

S-wave propagation from source to a high impedence contrast boundary can produce convert phase SP. Normally S-phases are recorded on radial component and SP-phase on vertical component. Using three component data, these two phases can be identified and isolated. Some significant structure information can be studied from these two phases. The Q value of sedimentary rock is one of them. The spectral ratio of SP- and S-phases are calculated in this study for estimating frequency-independent Q value of near surface layer. By the help of P- and S-waves velocity structure, the travel times of SP- and S-phases can be estimated such that SP-phase is identified. Three SP-phases, converted from different layers in the Lotung area, can be identified. The earliest SP-phase is possibly converted from the bottom of PLEISTOCENE formation. The second SP-phase might be converted from the bottom of ALLUVIUM layer, and the last one might be converted from the bottom of surface soil layer. Each SP/S ratio gives a different Q value which shows the variation of Q in each layer. The range of Q value estimated by this method agreed with the laboratory measurement of sedimentary rock.

1. INTRODUCTION

The shape of Fourier amplitude spectrum of accelerograms has had many engineering applications (McGuire, 1978). The shape of high frequency spectrum contains information of earthquake source and wave propagation (Anderson and Hough, 1984). The study of Q can also be determined from the shape of high frequency spectrum. A more recent method using the spectrum ratio of SP- and S-phases to calculate the ratio of Q_p/Q_s in near surface layer is studied by Clouser and Langston (1991). The reason why estimating near surface Q value is so important is: (1) site effect causes waveform distortion and that makes source study difficult (2) stress induced fracture causes low Q value (3) high fluid saturation causes low Q value and this might be an indication of oil reservoir. However, Q value depends on wavetypes named Q_s and Q_p for the S- and P-wave respectively. There is some independent evidence, obtained in conjunction with seismic exploration techniques,

* Institute of Seismology National Chung Cheng University, Chiayi, Taiwan, R.O.C.

indicating that Q is independent of frequency in the shallow crust (Hauge, 1981). McDonal *et al.* (1958) concluded that both Q_p and Q_s are independent of frequency in Pierre Shale formation, Colorado. Tullos and Reid (1969) found $Q_p = 2$ over the depth range 1 to 10 feet in Gulf Coast sediments, and was 1 to 2 orders of magnitude at depths from 10 to 100 feet. Hamilton (1976) has summarized attenuation measurements as a function of depth in sea-floor sediment. Wong *et al.* (1983) find that attenuation is highly variable in the depth range 100 to 350 m. Joyner *et al.* (1976) find that $Q_s = 16$ applies to the upper 186 m of sediments for a site near San Francisco Bay, and Kurita (1975) find $Q_s = 20$ for the upper crust in the northeast of the San Andreas fault near Hollister. In laboratory measurements (sandstone), Johnston and Toksöz (1980) report Q_s is equal to or slightly greater than Q_p for dry sample. Winkler and Nur (1982) result of Q_s is markedly greater than Q_p for partial water saturation. Vassiliou *et al.* (1982) gave the general observations of $Q_p - Q_s$ relation in sedimentary rocks; $Q_p = Q_s$ for dry rocks, $Q_p \geq Q_s$ for fully saturated rocks, and $Q_p < Q_s$ for partial saturation.

Knowledge of low quality factor Q for P-wave (Q_p) and S-wave (Q_s) is evidently a typical phenomenon for the sedimentary rock.

2. METHODOLOGY

When an earthquake happens, S-waves propagate from source to a near surface boundary which is usually the bottom of sedimentary rock or basin with very high impedence contrast, therefore strong converting phase S to P (named SP) takes place. In this case, the SP phases will be recorded in vertical component and they could be identified in most cases as in this study. This kind of converting can take place in many layers in which impedence contrast is high.

A schematic diagram is illustrated in Figure 1 for the ray paths of S-P and S-S, which are marked by R1 and R2. Obviously, the ray paths of R1 and R2 traveling from source to the boundary are different, but the difference can be very small and is probably negligible. Based on this assumption, the ray-path effects of R1 and R2 are almost equal.

The Fourier amplitude spectrum of high frequency accelerograms can be written as (Anderson and Hough, 1984):

$$A(f) = S(f)G(f)R(f)e^{-\pi f t^*} \tag{1}$$

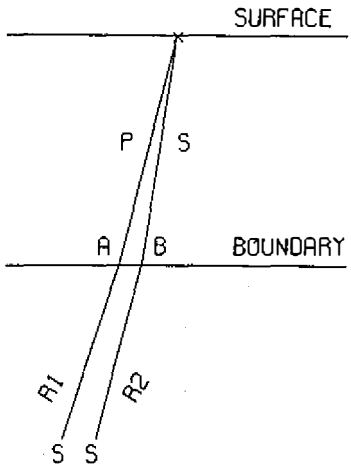

Fig. 1. Ray paths of S convert to P (R1) and S to S (R2) at points A and B of the boundary respectively.

where A(f) is recorded Fourier amplitude spectrum, S(f) is source spectrum, G(f) is ray-path effects, R(f) is receiver function, and t^* is travel time divided by quality factor

If we are able to isolate S- and SP-phases from the accelerograms, then their Fourier amplitude spectra can be calculated separately for S- and SP-phases. Following equation (1), their corresponding spectrum can be written in the form of

$$A_s(f) = S(f)G_1(f)T_sR(f)e^{-\pi f t_s/Q_s} \tag{2}$$

$$A_{sp}(f) = S(f)G_2(f)T_{sp}R(f)e^{-\pi f t_{sp}/Q_p} \tag{3}$$

$A_s(f)$ and $A_{sp}(f)$ are Fourier amplitude spectra of S-phase and SP-phase respectively. $G_1(f)$ and $G_2(f)$ are ray-path effects of R2 and R1 from source to the boundary. T_s and T_{sp} are the transmitting coefficients of S to S and S to P at points B and A (Figure 1) respectively. According to previous assumption that the ray path effects are equal, $G_1(f)$ is equal to $G_2(f)$. The sign t_s and t_{sp} are the travel times of S and P from the boundary to the receiver. The quality factors Q_s and Q_p correspond to S- and SP-phases attenuation in this sedimentary layer.

Dividing equation (3) by (2), we obtain spectral ratio of SP/S in this layer. Taking Logorithm on both side, we get the following equation as shown in Clouser and Langston (1991).

$$Log(\frac{A_{sp}(f)}{A_s(f)}) = Log(\frac{T_{sp}}{T_s}) + \pi f(\frac{t_s}{Q_s} - \frac{t_{sp}}{Q_p}) \tag{4}$$

If we plot the Logorithm spectral ratio with frequency f which is $Log - Linear$ plot, then equation (4) is a straight line with intercept (itc) and slope (m) where itc and m are listed below:

$$itc = Log(\frac{T_{sp}}{T_s}) \tag{5}$$

$$m = \pi(\frac{t_s}{Q_s} - \frac{t_{sp}}{Q_p}) \tag{6}$$

The intercept contains information about velocity and density above and below the boundary as well as incident angles of R1 and R2 at the boundary. Unfortunately, there are not enough messages to solve these parameters so that they are not interpreted at this study. The slope m contains the information of attenuation and travel time of S- and SP-phases in the shallow layer. The four parameters, t_s, t_{sp}, Q_s, and Q_p, can not be solved independently by equation (6). With the help of forward modeling under the conditions of accurate source location and well-known velocity structure, the ratio of Q_p/Q_s can be determined (Clouser and Langston, 1991). The quality factors Q_p and Q_s are equal in the case of dry rock according to measurement in the laboratory (Winkler and Nur 1979, 1982; Johnston and Toksöz 1980), or Q_p and Q_s are only slightly different if the rock contains a small fraction of fluid.

To solve equation (6), we have to assume that Q_s is equal to Q_p, and this solution will give a range of Q value roughly (no matter what kind of Q). This assumption is highly idealized. However, it can lead to the understanding of the range of quality factor for the sedimentary rock in the area of this study even though it is not the absolute value.

At this approximation, equation (6) can be rewritten as :

$$m = \pi(\frac{t_s - t_{sp}}{Q}) = \pi(\frac{\delta t}{Q}) \tag{7}$$

where δt is the travel time diffference of S and SP-phases travelling in the shallow layer. This time difference can be measured from the seismogram directly. Therefore, the estimated Q value can be expressed as

$$Q = \frac{\pi \delta t}{m} \tag{8}$$

This simple equation determines the quality factor from measuring time difference of S- and SP-phases and calculating the slope of $Log - Linear$ spectral ratio.

3. VELOCITY STRUCTURE AND PHASE IDENTIFICATION

The accelerograms used in this study are from the earthquake which occurred on July 30, 1986, at the time of 1131 UT, at epicenter 121°, 47.650′E, 24°, 37.728′N with depth 1.6 km, M_L= 6.2 and recorded by SMART-1 array. Twelve accelerograms recorded by inner array (station I01 to I12) are used and their relative station information is listed in Table 1.

Table 1

EARTHQUAKE: July 30, 1986, 1131UT

EPICENTER: 121°, 47.650′E, 24°, 37.728′N

M_L = 6.2, DEPTH = 1.6 Km

SMART-1 INNER STATIONS

Station Code	Longitude Degree	Latitude Degree	Epicenter Distance km	Azimuth Degree
I01	121.76503	24.67548	5.88317	329.9614
I02	121.76603	24.67503	5.88122	331.0793
I03	121.76663	24.67434	5.70828	330.8153
I04	121.76671	24.67336	5.64820	330.5714
I05	121.76620	24.67254	5.69070	330.2052
I06	121.76515	24.67206	5.71532	329.1285
I07	121.76419	24.67201	5.43725	326.1226
I08	121.76350	24.67428	5.59181	325.4115
I09	121.76277	24.67319	5.66325	325.9074
I10	121.76278	24.67410	5.76167	326.5683
I11	121.76346	24.67485	5.82538	327.8037
I12	121.76414	24.67550	5.93751	329.2470

The P-wave velocity structure of this area can be found in Wen and Yeh (1984), and detailed S-wave velocity structure can be found from HCK (1986). For easy reference, this

averaged velocity structure and their relative travel times are listed in Table 2. From Table 2, we can see that there could be three possible converting boundaries. One is the bottom of PLEISTOCENE formation in which S-wave velocity change from LUSHAN formation to PLEISTOCENE formation (750 m/s). The second boundary is the bottom of ALLUVIUM layer in which S-wave velocity changes from PLEISTOCENE (750 m/s) to ALLUVIUM (200 m/s) sharply. Another boundary is the bottom of surface soil in which S-wave velocity changes from ALLUVIUM (200 m/s) to soil (140 m/s). The converted SP also possibly takes place in the bottom of LUSHAN formation, but it is not clear for this data set. Estimating travel time difference between S- and SP-phases from relative velocity structure can help to identify SP-phase. The travel time difference between S-phase and SP-phase converted from the bottom of soil is about 0.082 second, and converted from the bottom of ALLUVIUM layer is about 0.30 second. These two converted phases are identified very well in obversed accelerograms, and their travel time differences are roughly consistent with calculated value. However, we do observe an earlier SP-phase that arrives before the former two SP-phases. By calculating the travel time difference ($\approx$ 0.462 second), this SP-phase might be converted from the bottom of PLEISTOCENE formation.

Table 2

VELOCITY STRUCTURE OF LOTUNG

Layer	Thickness m	V_p m/s	t_p second	V_s m/s	t_s second	δt second
SOIL	15	600	0.025	140	0.107	0.082
ALLUVIUM	50	1500	0.033	200	0.25	0.218
PLEISTOCENE	200	1900	0.1053	750	0.267	0.162
LUSHAN	?	3600	?	?	?	?

4. COMPUTATION PROCEDURE

1. Axis rotation: We consider anisotropic effect as negligible, though the SP-phase is mainly converted from SV instead of SH. The spectral ratio is calculated from SP and SV only. To avoid the disturbance from SH arrivals, the two horizontal seismograms (EW and NS directions) have to be rotated into radial and transverse direction by the calculation of azimuth angle (Table 1). After this rotation, SV- and SH-phases will be separated. Before being analyzed, all of the data used in this study have been rotated first.
2. Phases picking window: For the existence of near surface low velocity layer, ray path always refracts to nearly normal incidence (Figure 1). This phenomenon is particularly obvious for the first P-wave arrival so that it can be observed at the vertical component clearly, but the two horizontal components are almost invisible. Similarly, S converts to P and S to S also refracts to a vertical direction so that most energy of SP is recorded on the vertical component and S is recorded on the radial component. Due to this reason, we should select three windows on the vertical component for different SP-phases picking and another window followed by the first three on the radial component for S-phase picking. This selection is shown in Figure 2; note that S-phase is picked later

than other three SP-phases. A program (PICK) is designed to do this picking iteratively. The window used for S-phase is recommanded to contain all S wavetrain and to reject later coming surface wave. There are three windows used for SP-phases and separated by dash box windows. The SP-phases are identified in the vertical component; the range of each window is chosen by eyes.

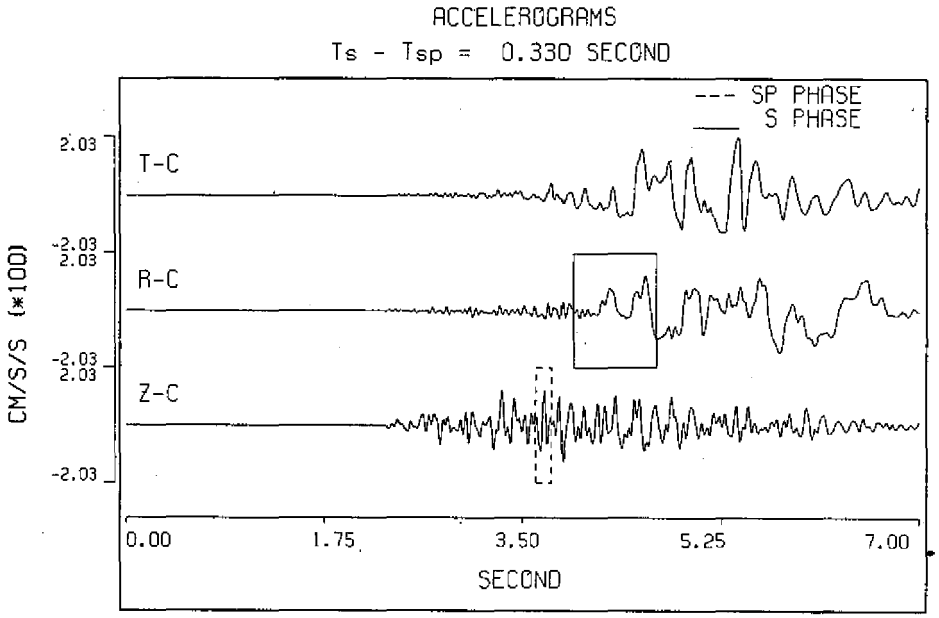

Fig. 2. Three-component accelerograms and windowed time series of SP- and S-phases. SP-phase is windowed in vertical component and S-phase in radial component respectively. The SP-phase is possiblly converted from the bottom of ALLUVIUM layer.

Once the box windows have been chosen, a half length cosine square taper is applied to each side of every box window. This procedure is neccessary to avoid spectral leakage (Jeffrey, 1987). Different tapers may be used but they cause no significant changes (Clouser and Langston, 1991). The travel time difference δt between S- and SP-phases is calculated from the beginning of these two windows.

3. Spectrum estimation: The windowed time series of S- and SP-phases are zero padding up to 512 points (5.12 seconds) and brought to frequency domain by taking FFT separately. Since a 25 Hz high cut filter had been applied to the instrument, the spectrum for frequency higher than 30 Hz is considered as background noise so that it would not be plotted. A smoothed procedure is applied to both Fourier amplitude spectra by a moving window with length 1.3672 Hz. As an example, the calculated smooth spectra are plotted together as shown in Figure 3-(a). In this Figure, the solid line is $Log - Linear$ plot of S-phase and the dashed line is SP-phase plot respectively. The

spectral ratio is also plotted in $Log - Linear$ scale such that the linear relation of equation (3) can be obtained by least square fitting over frequency range of interest which is 1.0 Hz to 22.0 Hz. There is a very few signals contained for frequency higher than 22.0 Hz in which S/N ratio is low. The spectral ratio is shown in Figure 3-(b), where the straight line is obtained from the least square fitting with slope and Q marked in the Figure.

The Q value is calculated from the slope of straight line and arrival time difference between S- and SP-phases. A program (QSP) is designed to perform the above calculation with changeable frequency range iteratively.

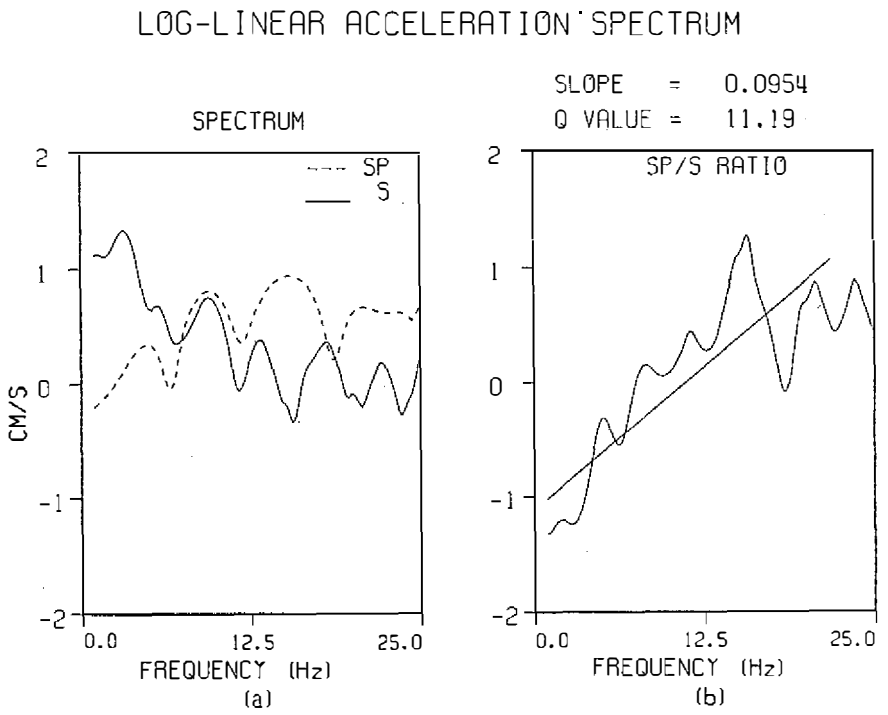

Fig. 3. Display spectra and spectral ratio of SP- and S-phases as windowed in Fig. 2. (a) Calculated spectra of SP- and S-phases (b) the spectral ratio of SP and S and straight line of the least square fitting (1 to 22Hz).

5. RESULTS

The data are ordered by respective station number. Three SP-phases converted from different boundary are picked for all accelerograms and shown in Figure 4. They are marked by three dashed rectangular boxes. The first box is the SP converted from the bottom of PLEISTOCENE formation, the second from the bottom of ALLUVIUM layer and the last from the bottom of soil layer. Every S-wave arrival for each station is windowed by dashed box as shown in Figure 5. Certainly, all the S-waves arrive after three SP-phases. Each

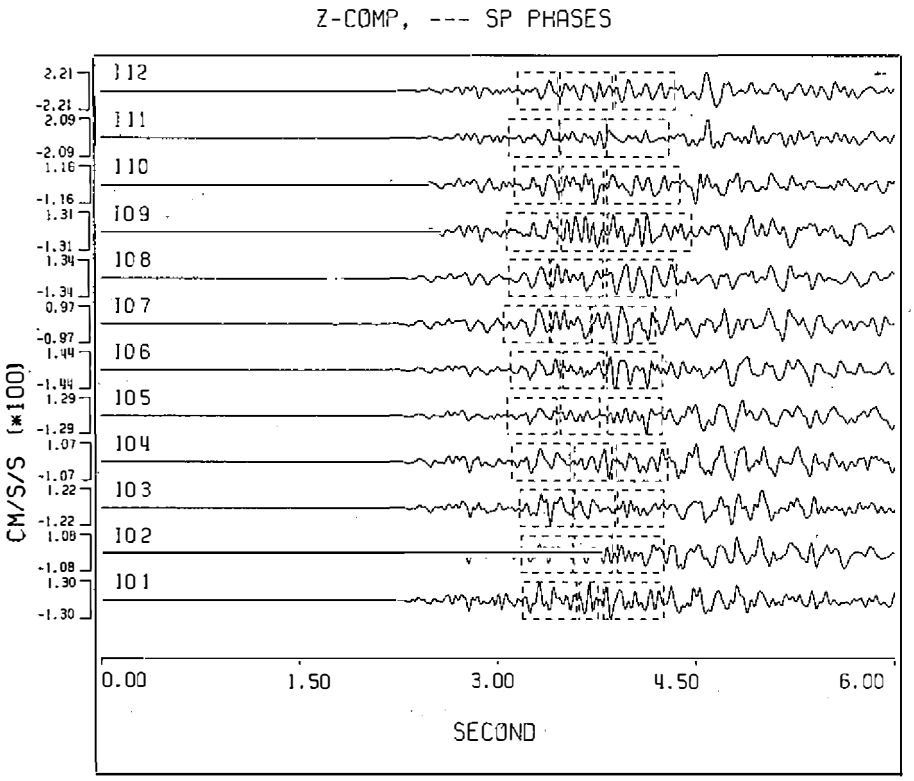

Fig. 4. Three SP-phases converted from different boundary are windowed in the vertical component for every stastion used in this study. The station numbers are marked in the beginning of each accelerogram. The first window is SP converted from the bottom of PLEISTOCENE formation, the second is from the bottom of ALLUVIUM layer and the last is from the bottom of Soil layer.

SP/S spectral ratio is calculated separately to show Q variation in each layer. First, the SP/S ratio is calculated for the case of converting from the bottom of soil layer. The spectral ratio results with Q value estimated are shown in Figure 6. The average Q value is 11.38 ± 6.26 which indicate very high attenuation in the soil layer. The second SP/S ratio results for SP converted from the bottom of ALLUVIUM formation are shown in Figure 7. Its' average Q value is 27.94 ± 10.93. This Q value is the total effect of alluvium and soil layers. The last SP/S ratio is calculated for the case of possiblly converting from the bottom of PLEISTOCENE formation. The results are shown in Figure 8. Its' average Q value is 55.11 ± 15.10. Similarly, it is the total effect of PLEISTOCENE formation, alluvium and soil layers. All of the Q values and δt are listed in Table 3 for reference and comparison. That Q value increased with depth of different formation is obvious.

The variation of Q values estimated from different stations can be assumed for the following reasons: (1) different site effect at the receiver (2) different crack density of ray

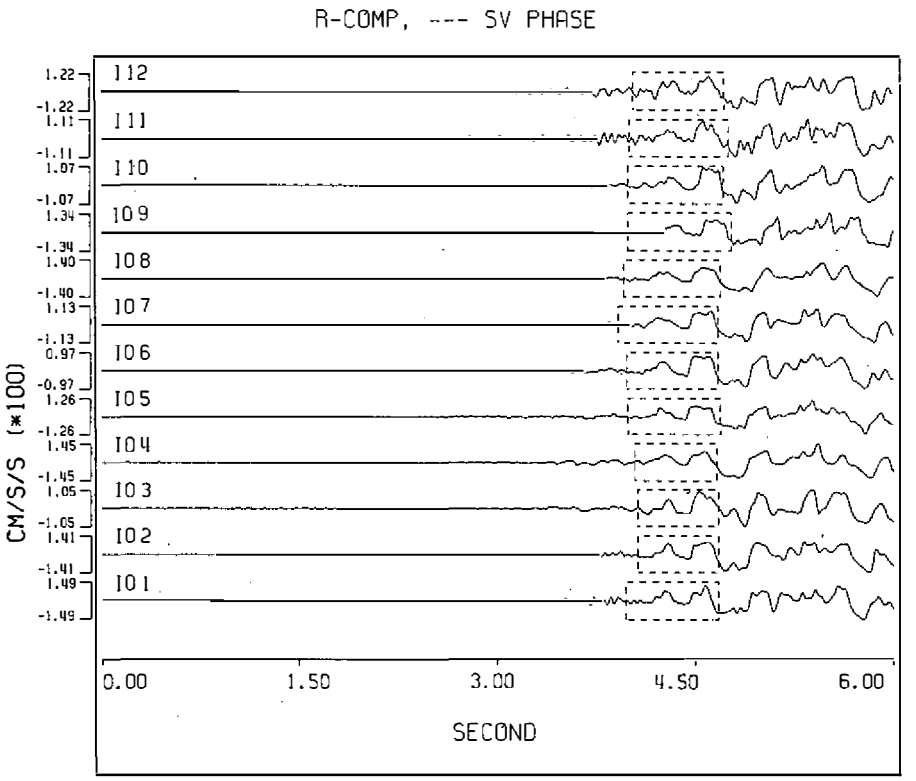

Fig. 5. The S-wave arrival followed by the three SP-phases is windowed in the radial component for every station.

path. Since all the stations are separated not too far, the maximum distance is 400 m (diameter), the variation is probably caused by site effect near the station.

The Q value of 11.38±6.26 of surface soil layer is very low, but acceptable (Tullos and Reid, 1969). The Q values of 27.94±10.93 and 55.11±15.10 of the other two cases are in the range of laboratory measurement for the sedimentary rock (Johnston and Toksöz, 1980). Hauksson *et al.* (1987) measured Q_p and Q_s in a borehole using vertically propagating waves from a nearby deep earthquake. They found a Q_p and Q_s of 44 and 25 respectively, between 420 and 1500m. However, the range of Q_p and Q_s depends on geological condition. It generally varies from about 10 to 100 for soft shale to very compact sedimentary rock.

The estimated Q value of this study is not Q_p nor Q_s unless the sedimentary rock is dry. This value simply gives us some idea about the range of Q_p and Q_s of local near surface sedimentary layer. They may not go too far from this estimated value.

6. DISCUSSION AND CONCLUSIONS

A simplified spectral ratio is designed to estimate near surface Q value of generally sedimentary rock by three SP- and S-phases. The converted phases of SP are probably taking

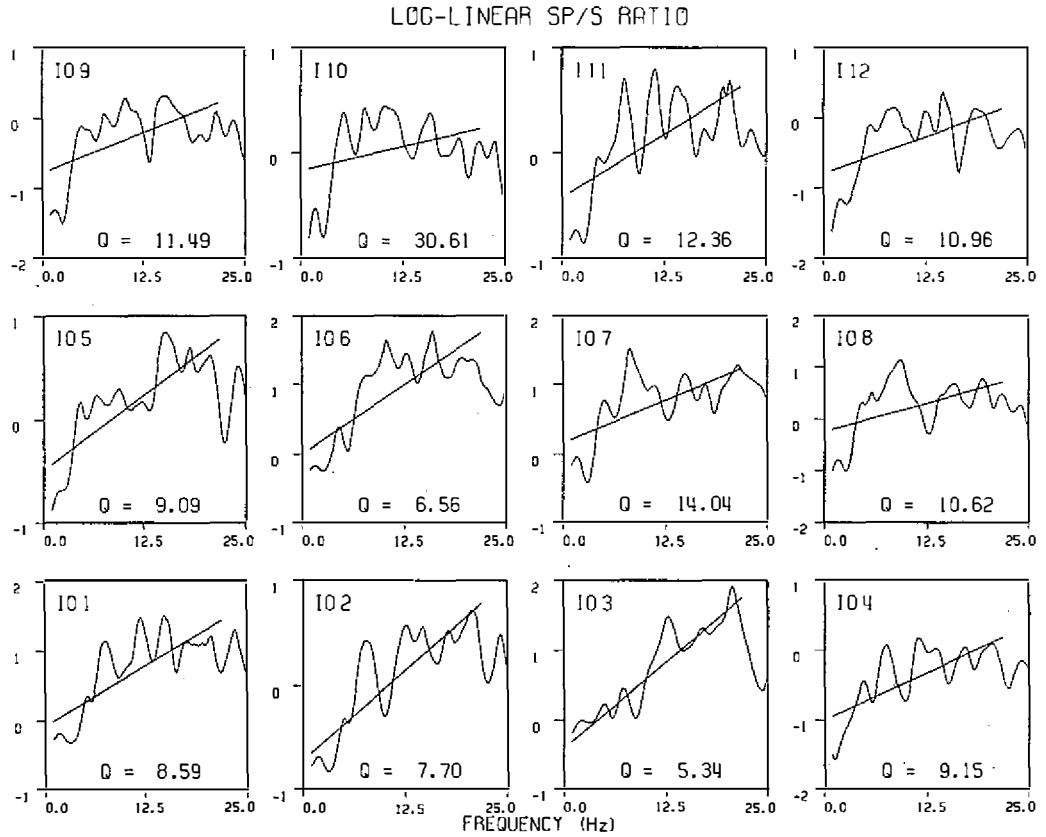

Fig. 6. Spectral ratio of SP/S and straight line of least square fitting (1 to 22Hz) of each station. This SP-phase is converted from the bottom of Soil layer. The station number is written on the top left and Q value is written on the bottom of each plot.

place at the boundary of high impedence contrast which is usually in sedimentary rock. For high crack density and fluid saturation rock (soil or others), particularly in oil gathered area, a very low Q is expected.

To estimate Q value, we need to assume $Q_p = Q_s$ though it is not really the case. However, this estimation gives us some idea about the variation and the range of Q values near the surface. The results show that very high attenuation (low Q) exists in the top 265 m of Lotung area.

Acknowledgements The author wish to thank Mr. Win-Gee Huang and Dr. Yih-Hsiung Yeh for collecting and sorting data. Special thanks belong to reviewers for their careful review and constructive suggestions. Dr. K.-L. Wen and Dr. Hung-Chie Chiu have helped me understand the characteristics of data in Lotung area; their generous offer is greately appreciated. The author would like to take this opportunity to thank the Institute of Earth Sciences, Academia Sinica for supplying data.

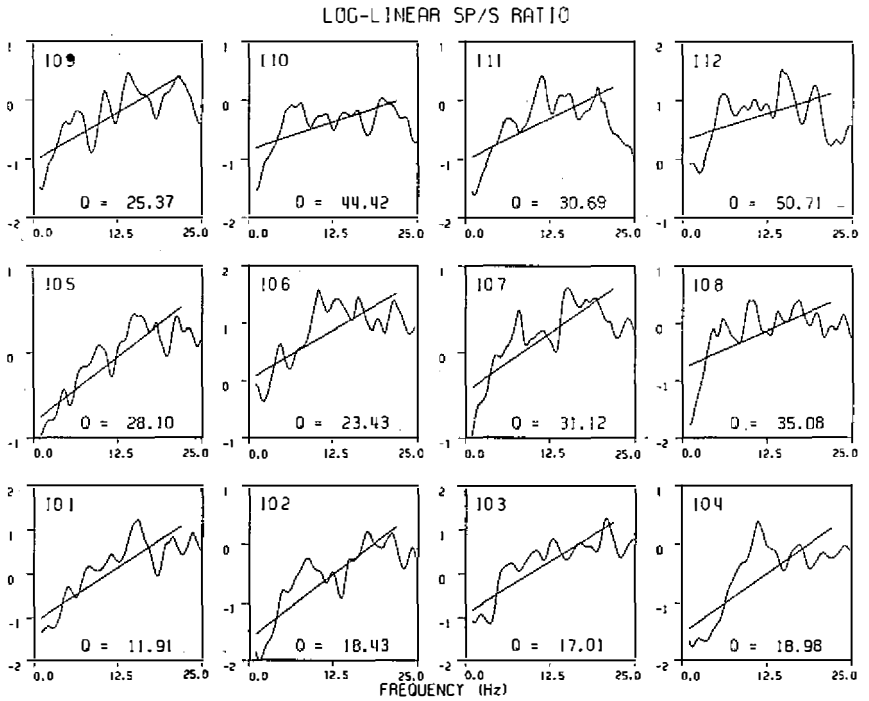

Fig. 7. Spectral ratio of SP/S and straight line of least square fitting (1 to 22Hz) of each station. This SP-phase is converted from the bottom of ALLUVIUM layer. The station number is written on the top left and Q value is written on the bottom of each plot.

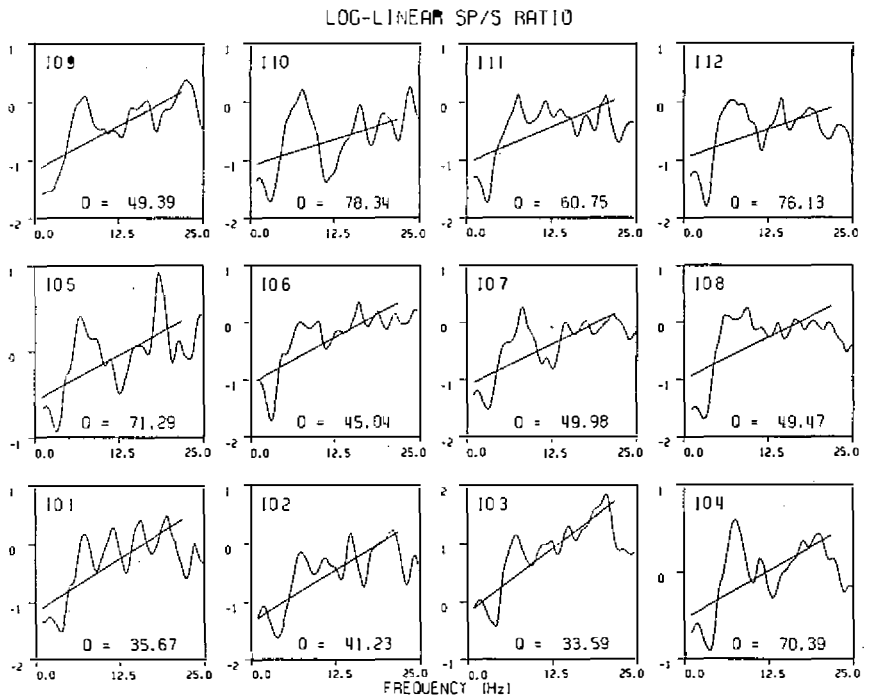

Fig. 8. Spectral ratio of SP/S and straight line of least square fitting (1 to 22Hz) of each station. This SP-phase is converted from the bottom of PLEISTOCENE formation. The station number is written on the top left and Q value is written on the bottom of each plot.

Table 3

δt AND Q-VALUE OF EACH BOUNDARY

Converting Boundary	Bottom of SOIL		Bottom of ALLUVIUM		Bottom of PLEISTOCENE	
Station Code	δt second	Q value	δt second	Q value	δt second	Q value
I01	0.075	8.59	0.165	11.91	0.380	35.67
I02	0.075	7.70	0.240	18.43	0.440	41.23
I03	0.075	5.34	0.240	17.01	0.440	33.59
I04	0.060	9.15	0.220	18.98	0.455	70.39
I05	0.075	9.09	0.255	28.10	0.455	71.29
I06	0.075	6.56	0.240	23.43	0.440	45.04
I07	0.050	14.04	0.205	31.12	0.385	49.98
I08	0.065	10.62	0.275	35.08	0.435	49.47
I09	0.075	11.49	0.250	25.37	0.460	49.39
I10	0.080	30.61	0.250	44.42	0.430	78.34
I11	0.085	12.36	0.260	30.69	0.455	60.75
I12	0.085	10.96	0.295	50.71	0.455	76.13
Average	0.073	11.38	0.241	27.94	0.436	55.11

REFERENCES

Anderson, J. G. and S. E. Hough., 1984: A model for the shape of the Fourier amplitude spectrum of acceleration at high frequency. *Bull. Seismol. Soc. Am.*, **74**, 1969-1993.

Clouser R.H. and C. A. Langston., 1991: $Q_p - Q_s$ relation in a sedimentary basin using converted phases. *Bull. Seismol. Soc. Am.*, **81**, 733-750.

Hamilton, E. L., 1976: Sound attenuation as a function of depth in the sea floor. *J. Acoust. Soc. Am.*, **59**, 528-535.

Hauge, P. S., 1981: Measurements of attenuation from vertical seismic profiles. *Geophysics*, **46**, 1548-1558.

Hauksson, E., T.-L. Teng, and T. L. Henyey., 1987: Results from a 1500m deep, 3-level downhole seismometer array: site response, low-Q values, and f_{max}. *Bull. Seismol. Soc. Am.*, **77**, 1883-1904.

HCK, 1986: Geophysical survey report of Lo-Tung project for Taiwan Power Company. *HCK Geophysical Company.*

Jeffrey, P., 1987: Multitaper spectral analysis of high-frequency seismograms. *J. Geophys. Res.*, **92,** 12675-12684.

Johnston, D. H. and M. N. Toksöz., 1980: Ultrasonic $P-$ and $S-$wave attenuation in dry and saturated rocks under pressure. *J. Geophys. Res.*, **85,** 925-936.

Joyner, W. B., R. E. Warrick, and A. A. Oliver. III, 1976: Analysis of seismograms from a downhole array in sediments near San Francisco Bay. *Bull. Seismol. Soc. Am.*, **66,**937-958.

Kurita, T., 1975: Attenuation of shear waves along the San Andreas fault zone in central California. *Bull. Seismol. Soc. Am.*, **65,** 277-292.

McDonal, F. J., F. A. Angona, R. L. Mills, R. L. Sengbush, R. G. Van Nostrand, and J. E. White., 1958: Attenuation of shear and compressional waves in Pierre Shale. *Geophysics*, **23,** 421-439.

McGuire, R. K., 1978: A simple model for estimating Fourier amplitude spectra of horizontal ground acceleration. *Bull. Seismol. Soc. Am.*, **69,** 803-822.

Tullos, F. N. and A. C. Reid., 1969: Seismic attenuation of Gulf coast sediments. *Geophysics*, **34,** 516-528.

Vassiliou, M., C. A. Salvado, and B. R. Tittmann., 1982: Seismic Attenuation, in CRC *Handbook of Physical Properties of Rock*, vol. III, R. S. Carmichael (Editor), CRC Press, Boca Raton, Florida.

Wen, K.-L. and Y. T. Yeh., 1984: Seismic velocity structure beneath the SMART 1 array. *Bull. Inst. Earth Sci., Academia Sinica*, **4,** 51-72.

Winkler, K. and A. Nur., 1979: Pore fluids and seismic attenuation in rocks. *Geophys Res. Lett.*, **6,** 1-4.

Winkler, K. and A. Nur., 1982: Seismic attenuation: effects of pore fluids and frictional sliding. *Geophysics*, **47,** 1-15.

Wong, J., P. Hurley, and G. F. West., 1983: Crosshole seismology and seismic imaging in crystalline rocks. *Geophys. Res. Letters.*, **10,** 686-689.

由SP/S譜比值估計Q值

謝 秋 霧
國立中正大學地震研究所

摘要

S波從震源傳播到高阻抗對照的邊界時，會產生轉換的波相SP。通常S波主要記錄在徑向分量，而SP波記錄在垂直分量，用三分量資料，這兩個波相可以識別並分離。而研究這兩個波相，可以得到構造上的一些訊息。沈積岩的Q值就是其中之一。本研究主要由計算SP/S的譜比值，估計近表層和頻率無關的Q值 。

藉由淺層P及S波的速度構造，SP及S波的走時可以估計，所以不同的SP波能被識別。在羅東地區，有三個從不同邊界轉換的SP波，可以被識別出來。最早到達的SP波是從更新世地層底部轉換，第二到達的SP波是從沖積層底部轉換，而最後到達的 SP 波則是從表層土壤底部轉換而來。從三個不同的SP/S譜比值，求出不同的Q值，顯示Q值在不同層的變化。此法估計之Q值，和實驗室內量度沈積岩之Q值符合 。